

Detection of virus-specific T cells and CD8⁺ T-cell epitopes by acquisition of peptide–HLA–GFP complexes: analysis of T-cell phenotype and function in chronic viral infections

UTANO TOMARU¹, YOSHIHISA YAMANO¹, MASAHIRO NAGAI², DRAGAN MARIC³,
PREVIN T.P. KAUMAYA⁴, WILLIAM BIDDISON¹ & STEVEN JACOBSON¹

¹Neuroimmunology Branch, National Institute of Neurological Disorders and Stroke,
National Institutes of Health, Bethesda, Maryland, USA

²Third Department of Internal Medicine, Faculty of Medicine, Kagoshima University, Kagoshima, Japan

³Laboratory of Neurophysiology, National Institute of Neurological Disorders and Stroke,
National Institutes of Health, Bethesda, Maryland, USA

⁴Department of Molecular and Cellular Biochemistry, Ohio State University, Columbus, Ohio, USA
U.T. and Y.Y. contributed equally to this work.

Correspondence should be addressed to S.J.; e-mail: jacobsons@ninds.nih.gov

Published online 24 March 2003; doi:10.1038/nm845

Antigen-specific CD8⁺ T cells acquire peptide–major histocompatibility complex (MHC) clusters through T-cell receptor (TCR)–mediated endocytosis after specific antigen stimulation. We generated an antigen-presenting cell (APC) expressing human leukocyte antigen (HLA)-A*201 coupled to the enhanced green fluorescent protein (GFP), which delivered GFP to an antigen-specific T cell when pulsed with antigenic peptide. We quantitatively identified human T-cell lymphotropic virus type I (HTLV-I) Tax(11–19) peptide–specific T-cell populations in peripheral blood mononuclear cells (PBMCs) from patients with HTLV-I–associated neurologic disease and defined a new CD8⁺ T-cell epitope in the HTLV-I envelope region. Acquisition of peptide–HLA–GFP complexes by antigen-specific T cells could distinguish, with respect to phenotype and perforin production, T cells from the chronic viral infections cytomegalovirus and HTLV-I. This approach will be a powerful tool in understanding the role of antigen-specific T-cell responses in health and disease.

Virus-specific T-cell responses are essential in host immune defense and have an important role in the pathogenesis of virus-mediated disorders. A crucial event in the initiation of an immune response is the activation of T lymphocytes through TCR recognition of the peptide–MHC, which initiates a precisely orchestrated cascade of molecular and cellular events. The detection and quantitative analysis of epitope-specific T-cell populations has been fundamental to our understanding of the cellular immune response in health and disease¹. Peptide–MHC clusters are acquired by CD8⁺ T cells and internalized through the TCR^{2,3}. Because this internalization is based on the specificity of peptide–MHC–TCR recognition, we postulated that acquisition of peptide–MHC molecules by T cells could be used for the quantitative detection of virus-specific T-cell populations, identification of viral T-cell epitopes and analysis of T-cell responses after antigen stimulation.

Here, we generate an APC expressing HLA-A*201 coupled to GFP (HmyA2GFP cells) and show that the acquisition of peptide–HLA–GFP complexes by antigen-specific T cells can quantitatively identify epitope-specific T cells and define new CD8⁺ T-cell immunodominant epitopes from bulk PBMCs. We also

use this system to characterize the phenotype and cytolytic function of virus-specific T cells in two chronic viral infections.

Acquisition of peptide–HLA–GFP complexes by CTL clones

To show antigen-specific acquisition of HLA–GFP complexes by CD8⁺ T cells, we used a CD8⁺ T-cell clone specific for the immunodominant HTLV-I Tax(11–19) peptide. HmyA2GFP cells (Fig. 1a) were pulsed with Tax(11–19) peptide and incubated with HTLV-I Tax(11–19)-specific cytotoxic T-lymphocyte (CTL) clones (Fig. 1b). Within 5 min, HLA–GFP molecules formed dense clusters at the T cell–APC contact site. After 30 min, small aggregates of HLA–GFP appeared within HTLV-I–specific CTL clones. The acquisition of peptide–HLA–GFP by T cells was also monitored by flow cytometry (Fig. 1c). After 30 min, most HTLV-I–specific CTL clones were positive for HLA–GFP but negative for the control human immunodeficiency virus (HIV) Gag(77–85) peptide. We also showed peptide-specific acquisition of HLA–GFP molecules by T cells using CTL clones specific for cytomegalovirus (CMV) pp65(405–503) peptide (Fig. 1c). To assess the kinetics of peptide–HLA–GFP acquisition by T cells, Tax(11–19)-specific CTL clones were incubated with Tax(11–19)-pulsed HmyA2GFP cells at various time points (Fig. 1d). After 30 min, most of the Tax(11–19)-specific CTLs were positive for HLA–GFP. Fluorescence level remained stable for 2 h and then declined. A dose-dependent titration of HTLV-I Tax(11–19)-pulsed HmyA2GFP cells resulted in a lower limit of detection of 100 pM peptide (data not shown).

Detection of virus-specific T cells from bulk PBMCs

Having observed that acquisition of peptide–HLA–GFP complexes can be readily detected in antigen-specific T-cell clones, we extended this system to identify and quantify antigen-specific T-cell populations from bulk PBMCs in patients with virus-associated diseases. We used PBMCs from HTLV-I-infected patients with an inflammatory disease of the central nervous system, known as HTLV-I–associated myelopathy and tropical spastic paraparesis (HAM/TSP)^{4,5}. HLA-A*201–positive patients show a high frequency of HTLV-I–specific CD8⁺ CTLs, most of which recognize the HTLV-I Tax(11–19) peptide^{6–8}. It has been suggested that these HTLV-I–specific CTLs have an

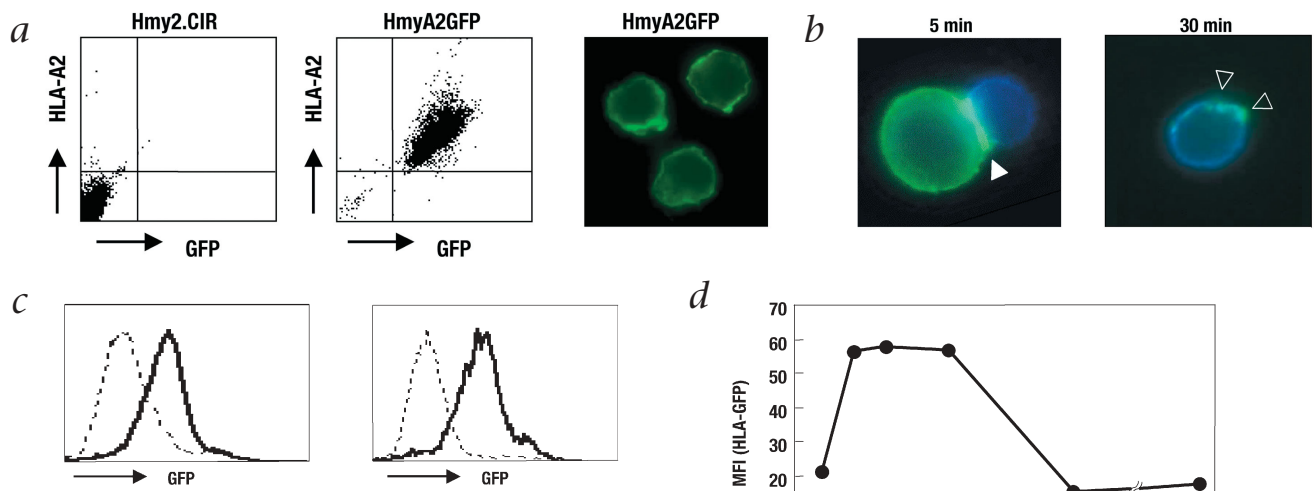


Fig. 1 Peptide-specific acquisition of peptide-HLA-GFP complexes by HTLV-I-specific CTL clones. **a**, Expression of HLA-A*201 molecule and GFP on HmyA2GFP cells. HLA-A*201 molecule and GFP were not expressed on untransfected Hmy2.CIR cells (left), but were colocalized on the transfected HmyA2GFP cells (center). The GFP signal on the transfected HmyA2GFP cells was also readily visualized by fluorescence microscopy (right). **b**, Peptide-HLA-GFP complexes acquired by HLA-A*201-restricted HTLV-I-specific CTL clone. The HmyA2GFP cells express GFP (green). The CTL clone is stained with an antibody against CD8 (blue). Within 5 min, HLA-GFP molecules formed dense clusters that could be readily visualized at the T cell-APC contact site (left, arrowhead). After 30 min, small aggregates of HLA-GFP appeared in the HTLV-I Tax(11-19)-specific CTL clone (right, arrowheads) where the majority of CD8⁺ cells that had acquired HLA-GFP were no longer in contact with the

HLA-GFP cells. **c**, Flow cytometric analysis of peptide-specific acquisition of peptide-HLA-GFP complexes by antigen-specific CTL clones. Both HTLV-I Tax(11-19)-specific (left) and CMV pp65-specific (right) CTL clones were positive for HLA-GFP (solid lines) but negative for the control HIV Gag(77-85) peptide (dotted line). **d**, Kinetics of peptide-HLA-GFP acquisition by CD8⁺ T-cell clone. The HTLV-I Tax(11-19)-specific CTL clone was incubated for the indicated periods with HmyA2GFP cells pulsed with Tax(11-19) peptide (●) or HIV Gag peptide (○). HLA-GFP acquisition by CTLs was directly analyzed by flow cytometry. HLA-GFP acquisition is expressed as mean fluorescence intensity (MFI).

important role in the pathogenesis of this disease^{7,9}. HmyA2GFP cells were pulsed with either HTLV-I Tax(11-19) or control HIV Gag(77-85) peptide and incubated with *ex vivo* PBMCs. The percentage of GFP⁺CD8⁺ cells from total PBMCs, as measured by flow cytometry, would then define the HTLV-I Tax(11-19)-specific T-cell population (Fig. 2). In HAM/TSP patient no. 4, relative to the control peptide, 25.13% of CD8⁺ cells were GFP-positive when incubated with HmyA2GFP cells pulsed with Tax(11-19) peptide (Fig. 2a). The frequency of Tax(11-19)-specific T cells in PBMCs from this patient was comparable to the frequency measured using HTLV-I Tax(11-19)-HLA-A*201 tetramers (28.21%; Fig. 2b). We further analyzed the frequencies of HTLV-I-specific T cells in PBMCs from eight HLA-A*201-positive HAM/TSP patients, three HLA-A*201-negative HAM/TSP patients and three HLA-A*201-positive healthy donors (Table 1). HTLV-I Tax(11-19)-specific T cells were detected in PBMCs from all patients at a frequency comparable with that of tetramers, but were not detected in HLA-A*201-negative patients or in healthy donors. We also used this A2GFP system for enumerating CMV-specific T cells in HAM/TSP patient no. 5 (Fig. 2c), again at a frequency comparable to that measured using CMVpp65-HLA-A*201 tetramers (Fig. 2d).

Detection of new CD8⁺ T-cell epitopes

We extended this system to detect previously unidentified antigen-specific CD8⁺ T cells by pulsing HmyA2GFP cells with a panel of peptides. We searched for HTLV-I envelope (Env)-specific CD8⁺ T cells from PBMCs of HAM/TSP patients. We incubated PBMCs from HLA-A*201-positive HAM/TSP patient no. 1

with HmyA2GFP cells pulsed with a series of 26 overlapping peptides from the HTLV-I Env gp46 region¹⁰ and analyzed HLA-GFP acquisition by CD8⁺ T cells using flow cytometry. Significant HLA-GFP acquisition by bulk CD8⁺ T cells was observed with the Env(291-305) peptide (Fig. 3a). To confirm this observation, we sorted the HLA-GFP-positive CD8⁺ T cells, a putative Env(291-305)-specific T-cell population, by flow cytometry (Fig. 3b) and assessed them for cytotoxicity using a variety of target cells (Fig. 3c). HTLV-I Env(291-305)-pulsed targets were lysed to a significant degree compared to control HTLV-I Env peptides. In addition, target cells infected with a vaccinia virus expressing HTLV Env and an autologous HTLV-I-infected CD4⁺ T-cell line (RS CD4) known to express HTLV-I¹¹ were also lysed by the Env(291-305)-sorted CD8⁺ T cells. These results showed that the sorted Env(291-305)-specific CD8⁺ T cells detected by the A2GFP system were peptide-specific and functionally cytolytic and indicated that the Env(291-305) region of HTLV-I might contain an immunodominant, HLA-A*201-specific CTL epitope. This Env(291-305) region contains a relatively strong HLA-A*201 binding motif¹², based on an estimation of the dissociation rate of the peptide-HLA complex (http://bimas.dcrt.nih.gov/molbio/hla_bind/).

Characterization of HTLV-I- and CMV-specific T cells

Differentiation phenotype and perforin production of virus-specific CD8⁺ T cells vary among persistent viral infections, which may be a result of the different functional properties necessary to control each virus during the chronic stage of infection^{13,14}. PBMCs from patients with HAM/TSP have high HTLV-I viral loads in the presence of large numbers of HTLV-

I-specific CTLs, suggesting that HTLV-I-specific T cells may be insufficient to control a persistent HTLV-I infection^{7,9}. In contrast, other chronic viral infections such as CMV elicit a highly effective and efficient CTL response associated with rapid clearance of the virus. This led us to compare the differentiation phenotype and perforin expression of HTLV-I- and CMV-specific T cells using PBMCs from HAM/TSP patients. In addition, T-cell responses after the recognition of peptide-HLA complexes are important for immune regulation during the chronic stage of viral infections. Therefore, we also analyzed differentiation phenotype and perforin expression of T cells after *ex vivo* peptide presentation by HmyA2GFP cells.

We first analyzed the distribution of the T-cell differentiation markers CD27 and CD45RA on HTLV-I Tax(11–19) tetramer-positive T cells and on CMV pp65 tetramer-positive T cells using PBMCs from HAM/TSP patients (Fig. 4a and b). CD27 and CD45RA molecules have been reported to distinguish phenotypic subpopulations of CD8⁺ T cells¹⁵. On the basis of both phenotypic and functional maturation properties, four distinct T-cell subsets have been described¹⁵: CD27⁺CD45RA⁺ (naive), CD27⁺CD45RA⁻ (memory), CD27⁻CD45RA⁻ (effector/memory), and CD27⁻CD45RA⁺ (effector). Although virus-specific populations during persistent HTLV-I infection were represented in each of the four phenotypic subsets, HTLV-I Tax(11–19) tetramer-positive T cells showed a clear enrichment for the CD27⁺CD45RA⁻ (memory) subset (Fig. 4a). By contrast, CMV tetramer-positive T cells showed a substantial enrichment for the CD27⁻CD45RA⁺ (effector) subset (Fig. 4b).

To study how virus-specific T cells with different phenotypes respond to antigen stimulation, we analyzed alterations of CD27 and CD45RA expression in HLA-GFP-acquiring HTLV-I- and CMV tetramer-positive T cells after *ex vivo* peptide presentation by HmyA2GFP cells (Fig. 4c and d). PBMCs from HAM/TSP patients were incubated with HTLV-I Tax(11–19) or CMV pp65 peptide-pulsed HmyA2GFP cells for 1 h, stained with antibodies against CD27 and CD45RA and with HTLV-I or CMV tetramers, and analyzed by flow cytometry. After stimulation with Tax(11–19)-pulsed HmyA2GFP cells, there was a decrease in the CD27⁺CD45RA⁻ (memory) subset and an increase in the CD27⁻CD45⁺ (effector) subset in HLA-GFP-acquiring HTLV-I tetramer-positive cells (Fig. 4c). In contrast, in HLA-

Table 1 Frequency of HTLV-I Tax(11–19)-specific, HLA-GFP-acquiring CD8⁺ T cells and tetramer-positive CD8⁺ T cells in HAM/TSP patients and healthy donors

Patient	% GFP acquisition ^a	% tetramer ^a
A201 ⁺ HAM no. 1	11.89	16.15
A201 ⁺ HAM no. 2	1.66	1.87
A201 ⁺ HAM no. 3	15.44	20.40
A201 ⁺ HAM no. 4	25.13	28.21
A201 ⁺ HAM no. 5	3.91	4.77
A201 ⁺ HAM no. 6	1.18	1.18
A201 ⁺ HAM no. 7	2.50	2.76
A201 ⁺ HAM no. 8	1.69	1.78
A201 ⁻ HAM no. 9	0.59	0.32
A201 ⁻ HAM no. 10	0.48	0.15
A201 ⁻ HAM no. 11	0.51	0.12
A201 ⁺ HD no. 1	0.43	0.12
A201 ⁺ HD no. 2	0.37	0.15
A201 ⁺ HD no. 3	0.33	0.13

^aPercentage of HLA-GFP- or tetramer-positive CD8⁺ cells in total CD8⁺ cells within PBMCs. HAM, HTLV-I-associated myelopathy and tropical spastic paraparesis; HD, HTLV-I-seronegative healthy donor; A201⁺, HLA-A*201-positive individual; A201⁻, HLA-A*201-negative individual.

GFP-acquiring CMV tetramer-positive T cells, there was no significant change in the proportion of effector T cells after stimulation with CMV pp65-pulsed HmyA2GFP cells (Fig. 4d). There was, however, a substantial increase in the CD27⁻CD45RA⁻ (effector/memory) subset with a concomitant decrease in the CD27⁺CD45RA⁻ (memory) subset (Fig. 4d).

These phenotypically defined T-cell populations were further characterized with respect to perforin expression and cytolytic activity. Our results were consistent with previous reports showing that terminally differentiated effector cells contain more perforin than cells with a naive or memory phenotype¹⁴. We showed that CMV-specific CD8⁺ T cells had higher levels of perforin than HTLV-I-specific CD8⁺ T cells *ex vivo* (Fig. 4e). In contrast, there was no change in the amount of perforin in HTLV-I-specific T cells after Tax(11–19) stimulation, and there was a significant decrease in the amount of perforin in CMV-specific T cells after CMVpp65 peptide stimulation ($P = 0.0166$ by paired T-test). These observations were supported by assessments of cytotoxicity in sorted HTLV-

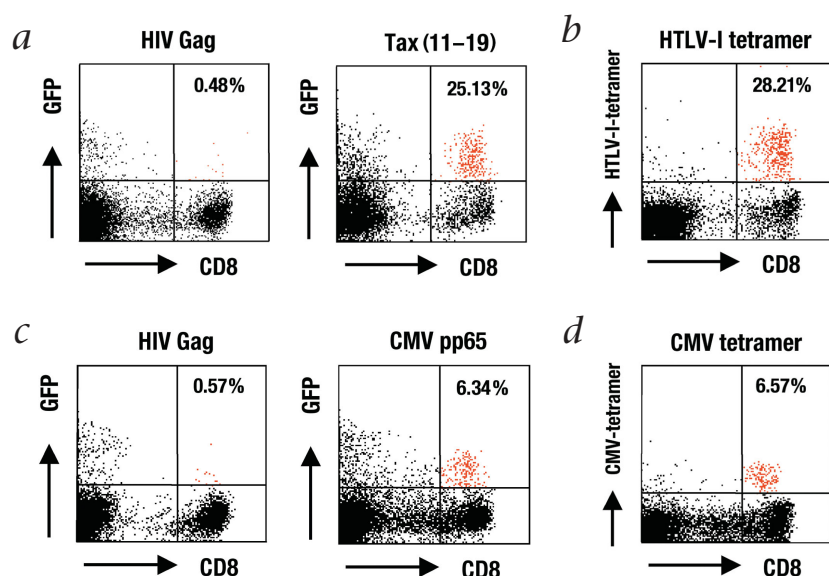
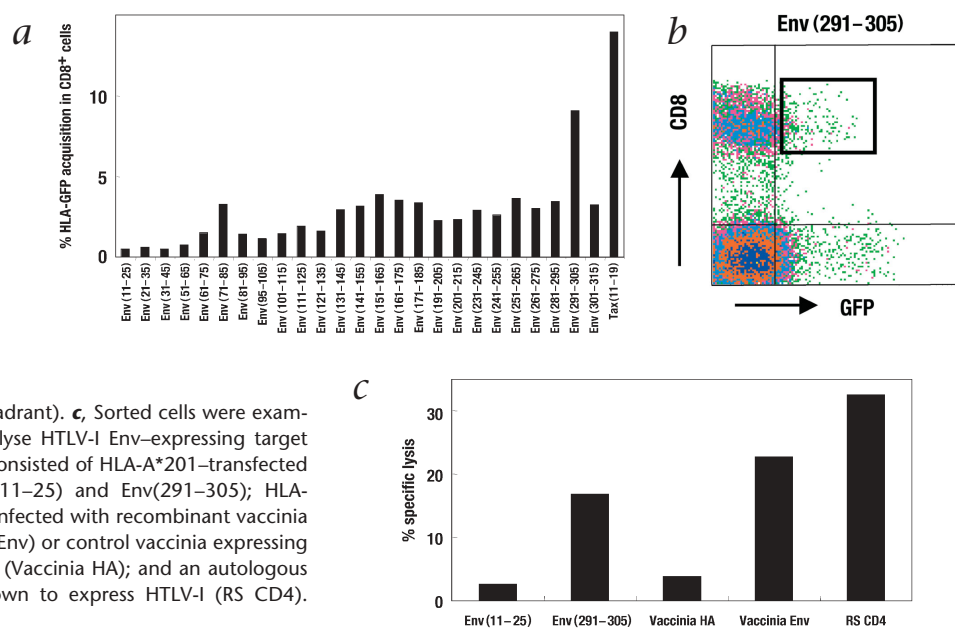


Fig. 2 Quantitative detection of virus-specific CD8⁺ T cells from bulk PBMCs of HLA-A*201-positive HAM/TSP patients. **a**, Representative dot plot of Tax(11–19)-specific HLA-GFP acquisition by CD8⁺ T cells from bulk PBMCs of HLA-A*201-positive HAM/TSP patient no. 4, with negative control HIV Gag(77–85) (left) or HTLV-I Tax(11–19) (right) peptides. The percentages of HLA-GFP-positive CD8⁺ T cells in total CD8⁺ cells are shown in red in the upper right quadrant. **b**, The percentage of HTLV-I Tax(11–19)-HLA-A*201 tetramer-positive cells in total CD8⁺ PBMCs from HAM/TSP patient no. 4 is shown in red in the upper right quadrant. **c**, Representative dot plot of CMV pp65-specific HLA-GFP acquisition by CD8⁺ T cells from bulk PBMCs of HLA-A*201 HAM/TSP patient no. 5, with negative control HIV Gag(77–85) (left) or CMV pp65 (right) peptides. **d**, Percentage of CMV pp65-HLA-A*201 tetramer-positive cells in total CD8⁺ PBMCs from HAM/TSP patient no. 5 is shown in red in the upper right quadrant.

Fig. 3 Detection of a new CD8⁺ T-cell epitope from the envelope region of HTLV-I. **a**, Frequency of HLA-GFP–positive CD8⁺ cells from bulk PBMCs that are reactive to HTLV-I peptides. Each peptide is designated by the position of its amino acid sequence. **b**, After the incubation of Env(291–305)-pulsed HmyA2GFP cells with PBMCs from HLA-A*201–positive HAM patient no. 1, cells were stained with a CD8-specific monoclonal antibody and HLA-GFP–acquiring CD8⁺ T cells were sorted by flow cytometry (inset, upper right quadrant). **c**, Sorted cells were examined for their functional capacity to lyse HTLV-I Env–expressing target cells in a 4-h CTL assay. Target cells consisted of HLA-A*201–transfected human B-cell line pulsed with Env(11–25) and Env(291–305); HLA-A*201–transfected human B-cell line infected with recombinant vaccinia virus expressing HTLV-I Env (Vaccinia Env) or control vaccinia expressing influenza virus hemagglutinin protein (Vaccinia HA); and an autologous HTLV-I–infected CD4⁺ T-cell line known to express HTLV-I (RS CD4). Effector/target ratio was 3:1.



I- and CMV tetramer–positive T cells. CMV tetramer–positive T cells induced higher cell lysis than HTLV-I tetramer–positive T cells (Fig. 4g); this was also observed in bulk, non-sorted PBMCs from a HAM/TSP patient (Fig. 4h).

Discussion

Antigen-specific T-cell interactions are important components of cellular immunity against microbial agents, self proteins and tumor antigens. The detection and quantitative analysis of epitope-specific T-cell populations has been important in understanding the cellular immune response in health and disease. Quantitative detection of T-cell populations by tetramers has proved useful for monitoring virus-specific T-cell immunity in laboratory and clinical settings¹. To generate the tetramers, however, requires *a priori* identification of an immunodominant peptide known to bind the appropriate MHC. During peptide-MHC recognition, membrane components of APCs containing MHC class I molecules are acquired by CD8⁺ T cells through the TCR^{2,3}. In the present study, we have exploited peptide-HLA acquisition by T cells for quantitative identification of antigen-specific T-cell populations from bulk PBMCs. Using the A2GFP system, HLA-A*201–restricted, HTLV-I– and CMV-specific CD8⁺ T cells were detected from bulk PBMCs of patients with HAM/TSP, at amounts and sensitivities comparable to those in tetramer detection (Table 1; Fig. 2). This system was also used to screen unknown CD8⁺ T-cell epitopes (Fig. 3). The A2GFP system has clear advantages over other antigen-specific T-cell screening methods (such as tetramers, Elispot and *in vitro* cytokine detection systems), as the HmyA2GFP cells stably express HLA-A*201–GFP and can be easily pulsed with any peptide in a 30-min incubation process. This straightforward method for constructing stably transfected HLA-GFP cells is also applicable with other HLA alleles. We feel this approach will be useful in the analysis of other infectious agents, tumors and auto-antigens and will further enhance our understanding of antigen–host cell immunological interactions.

The acquisition of peptide–HLA-GFP by T cells specific for HTLV-I or CMV was also used to define stages of T-cell differen-

tiation between two different chronic viral infections. To understand the T-cell immune response in persistent virus infections, virus-specific CD8⁺ T cells have been classified into distinct differentiation phenotypes using a combination of cell-surface markers such as CD27, CD28, CCR7, CD45RA and CD45RO, although these distinctions are primarily defined phenotypically and their correlations with function seem to be evolving^{13–15}. HIV-specific CD8⁺ T cells were enriched for T cells with a memory phenotype (pre-terminally differentiated) in addition to expressing low levels of perforin, whereas CMV-specific T cells were predominantly of an effector phenotype (terminally differentiated) with high levels of perforin^{13,14}. These results suggest that HIV-specific CD8⁺ T cells with an immature phenotype and a lack of perforin are associated with a defect in cytolytic activity that may contribute to the decline in CD8⁺ T-cell-mediated suppression of HIV replication and HIV disease progression¹³. In contrast, CMV-specific CD8⁺ cells with an effector phenotype and high perforin expression would be highly effective in eliminating CMV-infected cells¹³. Similar to the case in HIV, HTLV-I–specific T cells with a memory phenotype and low perforin are enriched in patients with HAM/TSP, a disorder in which immunopathogenic mechanisms have been proposed^{9,16}. In the same patients, CMV-specific T cells, which are highly effective in eliminating CMV-infected cells¹³, were predominantly of an effector phenotype with high levels of perforin. In patients with HAM/TSP, high HTLV-I viral loads in PBMCs have been seen in the presence of very high frequencies of HTLV-I–specific CTLs (as high as 25% of total CD8⁺ cells)⁸. Collectively, these results suggest that HTLV-I–specific T cells may be insufficient to control persistent HTLV-I infection.

The newly described A2GFP system allowed us to assess the response of virus-specific T cells after antigen recognition. Although it has been shown that heterogeneity exists within virus-specific T-cell populations^{13,14}, little is known about how virus-specific T cells with different phenotypes and levels of perforin expression respond to antigen when controlling viral infections. After antigen stimulation with peptide-pulsed HmyA2GFP cells, HTLV-I–specific CD8⁺ cells were enriched for

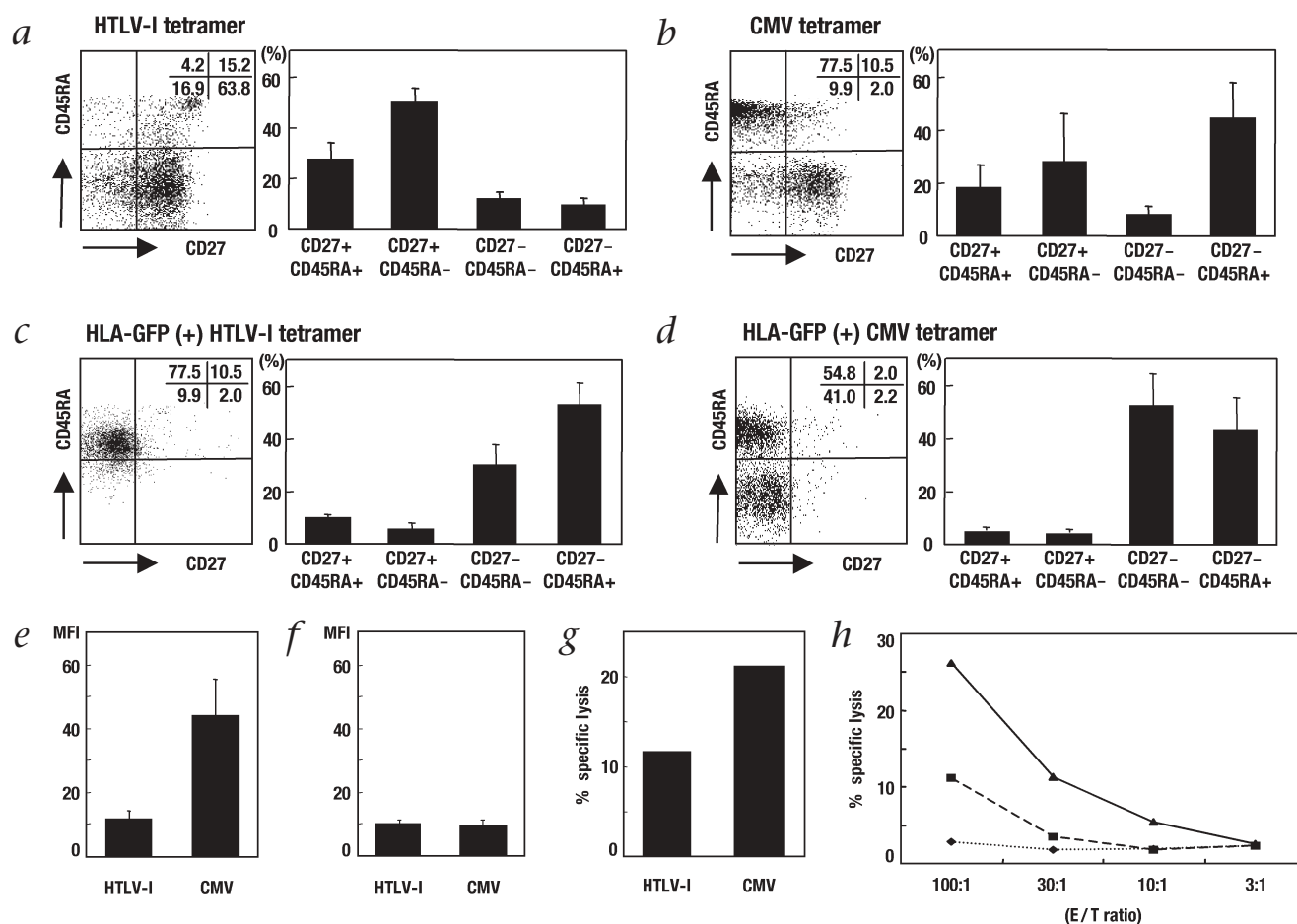


Fig. 4 Phenotypic and functional characterization of HTLV-I Tax(11–19)- and CMV pp65-specific T cells in PBMCs from HAM/TSP patients. **a–d**, Representative dot plots of CD27 and CD45RA expression on different subpopulations of PBMCs from HAM/TSP patient no. 5 (left panels). Bar graphs are the average of 7 HAM/TSP patients (*a* and *c*) or 4 HAM/TSP patients (*b* and *d*; right panels). Subpopulations were HTLV-I tetramer-positive cells (*a*), CMV tetramer-positive cells (*b*), HLA-GFP-acquiring HTLV-I tetramer-positive cells (*c*), and HLA-GFP-acquiring CMV tetramer-positive cells (*d*). Numbers at upper right represent the percentage of tetramer-positive cells within each quadrant. Data are mean \pm s.e.m. **e** and **f**, Intracellular perforin expression in HTLV-I- and CMV tetramer-positive cells (*e*) and

HLA-GFP-acquiring HTLV-I- and CMV-specific T cells (*f*) from 4 HAM/TSP patients. Data represent averaged mean fluorescence intensity (MFI; mean \pm s.e.m.). **g**, Cytolytic activity of tetramer-sorted T-cell populations. HTLV-I and CMV tetramer-positive cells were sorted by flow cytometry and examined for the functional capacity to lyse peptide-pulsed target cells in a 4-h CTL assay. Effector/target (E/T) ratio was 3:1. **h**, Cytolytic activity of bulk PBMCs from HAM/TSP patient no. 5. PBMCs from HAM/TSP patient no. 5 were examined for their functional capacity to lyse Tax(11–19)- or CMV pp65-pulsed target cells in a 4-h CTL assay at various E/T ratios. Specific lysis of non-peptide pulsed target cells by PBMCs was used as negative control. ◆, no peptide; ■, Tax(11–19); ▲, CMV pp65.

an effector phenotype without significant induction of perforin or increased cytolytic activity. These cells may be insufficient to control virus infection, resulting in increased viral load in HAM/TSP patients¹⁷. In the same patients, CMV-specific T cells, which are highly effective at eliminating CMV-infected cells¹³ after antigen stimulation, were enriched for cells with an effector or effector/memory phenotype, with high levels of cytolytic activity and rapid exhaustion of perforin. The generation of a recall antigen response is thought to be associated with the proliferation of memory cells and their conversion to effector cells¹⁸. It is therefore possible that terminally differentiated effector cells rapidly intervene after re-encountering antigen, while precursor cells expand and ensure continuous replenishment of the effector cell pool. Alternatively, differences in perforin expression between HTLV-I- and CMV-specific CD8⁺ T cells may be linked to their antigenic history *in vivo*. Various priming conditions (such as the abundance of antigen, the du-

ration of antigenic stimulation and the type of cytokine present)^{13,14,18} may be related to differences in the virus-specific T-cell phenotype and cytolytic function that are necessary to control chronic viral infection and disease outcome.

Acknowledgments

We thank K. Yao, S. Gagnon and S. Soldan for helpful comments, and R. Turner for help with flow cytometry. U.T. was supported by the Japanese Society for the Promotion of Science and a US National Institutes of Health Research Fellowship.

Competing interests statement

The authors declare that they have no competing financial interests.

- Altman, J.D. *et al.* Phenotypic analysis of antigen-specific T lymphocytes. *Science* **274**, 94–96 (1996).
- Huang, J.F. *et al.* TCR-mediated internalization of peptide-MHC complexes acquired by T cells. *Science* **286**, 952–954 (1999).

Methods

Generation of HmyA2GFP cells. The full-length *HLA-A*201* cDNA construct was obtained from the RSV-*HLA-A2* vector¹⁹. The *HLA-A2*-GFP expression vector was generated by insertion of the *HLA-A*201* cDNA with a stop codon mutated into the pEGFP-N3 vector (Clontech, Palo Alto, California). The *HLA-A* and *HLA-B* locus-defective immortalized B-cell line (Hmy2.CIR) was transfected with the *HLA-A2*-GFP vector using Trans-IT (Mirus, Madison, Wisconsin), according to the manufacturer's instructions. The cells were incubated for 48 h at 37 °C and placed in fresh selection medium DMEM (Gibco-BRL, Grand Island, New York) supplemented with 10% FBS (Atlanta Biologicals, Norcross, Georgia), 2 mM L-glutamine, 40 U/ml penicillin, 40 µg/ml streptomycin (all from BioWhittaker, Walkersville, Maryland) and 400 µg/ml of G418 sulfate (Cellgro, Herndon, Virginia) to establish a stable cell line (HmyA2GFP) expressing the *HLA-A*201*-GFP fusion protein (Fig. 1a).

Subjects. We used Ficoll-Hypaque (BioWhittaker) centrifugation to separate PBMCs from 8 *HLA-A*201*-positive HAM/TSP patients, 3 *HLA-A*201*-negative HAM/TSP patients and 3 *HLA-A*201*-positive HTLV-I-seronegative healthy donors. HAM/TSP was diagnosed according to the World Health Organization's guidelines²⁰. Blood samples were obtained after informed consent as part of a clinical protocol reviewed and approved by the National Institutes of Health institutional review panel. HTLV-I infection was confirmed by ELISA (Abbott Laboratories, Chicago, Illinois) and western blot analysis (Genelabs, Singapore).

Peptides. HTLV-I Tax(11–19) (LLFGYPVYV), HIV Gag(77–85) (SLYNTVATL) and CMV pp65 (495–503) (NLVPMVATV) peptides were synthesized and 95% purified by high-performance liquid chromatography (New England Peptide, Fitchburg, Massachusetts).

Generation of virus peptide-specific CTL clones. Previously characterized CD8⁺ CTL clones²¹ were used in these studies. They were maintained by weekly stimulation with peptide-pulsed (1 µM) irradiated *HLA-A*201*-allogeneic PBMCs at a CTL clone/PBMC ratio of 1:10. Human recombinant interleukin-2 (40 U/ml; Roche Diagnostic, Indianapolis, Indiana) was added on the next day of stimulation. CTL culture medium was Iscove's modified Dulbecco's medium (Gibco-BRL) supplemented with 10% human serum, 2 mM L-glutamine, 40 U/ml penicillin and 40 µg/ml streptomycin.

Immunofluorescence staining. HmyA2GFP cells were pulsed with HTLV-I Tax(11–19) peptide at a concentration of 10 µM for 30 min, and cultured with an HTLV-I Tax(11–19)-specific CD8⁺ T-cell clone for indicated periods on poly-D-lysine-treated glass coverslips at 37 °C. The cells were fixed in 4% paraformaldehyde and stained with monoclonal antibody against CD8 (DAKO,

Glostrup, Denmark) in combination with Alexa Fluor 350-conjugated goat antibodies against mouse IgG1 (blue; Molecular Probes, Eugene, Oregon). Images were examined with a Zeiss Axiovert 200M microscope.

Flow cytometric analysis. HmyA2GFP cells were pulsed with each peptide and incubated in a round-bottom 96-well culture plate for 30 min at 37 °C. The cells were washed twice to remove any free peptide, mixed with CTL clones (at a 1:5 HmyA2GFP cell/CTL ratio) or PBMCs (at a 1:1 ratio) in a round-bottom, 96-well culture plate, centrifuged at 200g for a few seconds to provide immediate cell contact and incubated for 30 min at 37 °C. Cells were then stained with a variety of antibodies (see below) and the acquisition of *HLA-GFP* by T cells was assessed by flow cytometry. CTL clones were stained with phycoerythrin-labeled monoclonal antibody against CD8 (Caltag, Burlingame, California) to detect *HLA-GFP* molecules. PBMCs were stained with Tri-Color-labeled monoclonal antibody against CD8 (Caltag) and phycoerythrin-conjugated Tax(11–19) peptide-loaded *HLA-A*201* tetramer (National Institutes of Health AIDS Research and Reference Reagent Program) or CMV pp65 peptide-loaded *HLA-A*201* tetramer (Beckman Coulter, Fullerton, California). For phenotypic analysis of PBMCs, cells were stained with phycoerythrin-conjugated Tax(11–19) peptide-loaded *HLA-A*201* tetramer, monoclonal antibody against CD27 and allophycocyanin-labeled monoclonal antibody against CD45RA. Peridinin chlorophyll protein-labeled rat antibody against mouse IgG1 was used as a secondary reagent for CD27-specific antibody (all from Pharmingen, San Diego, California). Cells were stained with saturating concentrations of antibody at 4 °C for 30 min and washed twice before analysis on a FACS Calibur (Becton Dickinson, San Jose, California). For intracellular perforin staining, cells were fixed and permeabilized with the Cytofix/CytoPerm kit (Pharmingen) and stained with monoclonal antibody specific for perforin (Pharmingen). Data were analyzed with CellQuest software (Becton Dickinson).

Cell sorting and CTL assay. Effector cells were sorted by a FACS Vantage SE (Becton Dickinson). The sorted cells were incubated in CTL culture medium (see 'Generation of virus peptide-specific CTL clones' above) overnight. The 4-h CTL assay was done using europium (Aldrich Chemical, Milwaukee, Wisconsin) as described previously²¹. Effector cells were incubated with target cells at indicated effector-to-target ratios. Target cells were from an *HLA-A*201*-transfected human B-cell line pulsed with 100 nM each Env(11–25), Env(291–305), Tax(11–19) and CMV pp65 peptide; an *HLA-A*201*-transfected human B-cell line infected with vaccinia recombinant viruses expressing HTLV-I Env or control vaccinia expressing influenza virus hemagglutinin protein; or an autologous HTLV-I-infected CD4⁺ T-cell line known to express HTLV-I (RSCD4)¹¹. The percent specific lysis was calculated as (experimental release – spontaneous release) ÷ (maximum release – spontaneous release) × 100. The assay was done in triplicate.

- Stinchcombe, J.C., Bossi, G., Booth, S. & Griffiths, G.M. The immunological synapse of CTL contains a secretory domain and membrane bridges. *Immunity* **15**, 751–761 (2001).
- Gessain, A. *et al.* Antibodies to human T-lymphotropic virus type-I in patients with tropical spastic paraparesis. *Lancet* **2**, 407–410 (1985).
- Osame, M. *et al.* HTLV-I associated myelopathy, a new clinical entity. *Lancet* **1**, 1031–1032 (1986).
- Jacobson, S., Shida, H., McFarlin, D.E., Fauci, A.S. & Koenig, S. Circulating CD8⁺ cytotoxic T lymphocytes specific for HTLV-I pX in patients with HTLV-I associated neurological disease. *Nature* **348**, 245–248 (1990).
- Bangham, C.R. The immune response to HTLV-I. *Curr. Opin. Immunol.* **12**, 397–402 (2000).
- Yamano, Y. *et al.* Correlation of human T-cell lymphotropic virus type 1 (HTLV-1) mRNA with proviral DNA load, virus-specific CD8⁺ T cells, and disease severity in HTLV-1-associated myelopathy (HAM/TSP). *Blood* **99**, 88–94 (2002).
- Jacobson, S. Immunopathogenesis of human T cell lymphotropic virus type I-associated neurologic disease. *J. Infect. Dis.* **186** (suppl. 2), S187–S192 (2002).
- Frangione-Beebe, M. *et al.* Enhanced immunogenicity of a conformational epi-

- tope of human T-lymphotropic virus type 1 using a novel chimeric peptide. *Vaccine* **19**, 1068–1081 (2000).
11. Mendez, E. *et al.* Astrocyte-specific expression of human T-cell lymphotropic virus type 1 (HTLV-1) Tax: induction of tumor necrosis factor α and susceptibility to lysis by CD8⁺ HTLV-1-specific cytotoxic T cells. *J. Virol.* **71**, 9143–9149 (1997).
 12. Parker, K.C., Bednarek, M.A. & Coligan, J.E. Scheme for ranking potential HLA-A2 binding peptides based on independent binding of individual peptide side-chains. *J. Immunol.* **152**, 163–175 (1994).
 13. Champagne, P. *et al.* Skewed maturation of memory HIV-specific CD8 T lymphocytes. *Nature* **410**, 106–111 (2001).
 14. Appay, V. *et al.* Memory CD8⁺ T cells vary in differentiation phenotype in different persistent virus infections. *Nat. Med.* **8**, 379–385 (2002).
 15. Hamann, D. *et al.* Phenotypic and functional separation of memory and effector human CD8⁺ T cells. *J. Exp. Med.* **186**, 1407–1418 (1997).
 16. Osame, M. Pathological mechanisms of human T-cell lymphotropic virus type I-associated myelopathy (HAM/TSP). *J. Neurovirol.* **8**, 359–364 (2002).
 17. Nagai, M. *et al.* Analysis of HTLV-I proviral load in 202 HAM/TSP patients and 243 asymptomatic HTLV-I carriers: high proviral load strongly predisposes to HAM/TSP. *J. Neurovirol.* **4**, 586–593 (1998).
 18. Sallusto, F., Lenig, D., Forster, R., Lipp, M. & Lanzavecchia, A. Two subsets of memory T lymphocytes with distinct homing potentials and effector functions. *Nature* **401**, 708–712 (1999).
 19. Winter, C.C., Carreno, B.M., Turner, R.V., Koenig, S. & Biddison, W.E. The 45 pocket of HLA-A2.1 plays a role in presentation of influenza virus matrix peptide and alloantigens. *J. Immunol.* **146**, 3508–3512 (1991).
 20. Osame, M. Review of WHO Kagoshima meeting and diagnostic guidelines for HAM/TSP. in *Human Retrovirology HTLV* (ed. Blattner, W.) 191–197 (Raven Press, New York, 1990).
 21. Kubota, R., Soldan, S.S., Martin, R. & Jacobson, S. An altered peptide ligand antagonizes antigen-specific T cells of patients with human T lymphotropic virus type I-associated neurological disease. *J. Immunol.* **164**, 5192–5198 (2000).